HHS Public Access

Author manuscript

Cardiol Clin. Author manuscript; available in PMC 2017 February 01.

Published in final edited form as:

Cardiol Clin. 2016 February ; 34(1): 47–57. doi:10.1016/j.ccl.2015.08.003.

Automated Quantitative Nuclear Cardiology Methods

Manish Motwani, PhD,
Advanced Cardiac Imaging Fellow, Cedars-Sinai Medical Center, 8700 Beverly Blvd, Los Angeles, CA 90048, Tel: (310) 423-4348, manish.motwani@cshs.org

Daniel S. Berman, MD,
Departments of Imaging and Medicine, Cedars-Sinai Medical Center, Los Angeles, CA, bermand@cshs.org

Guido Germano, PhD, and
Departments of Imaging and Medicine, Cedars-Sinai Medical Center, Los Angeles, CA, guido.germano@aim.cshs.org

Piotr J. Slomka, PhD
Scientist, Artificial Intelligence in Medicine Program, Professor of Medicine, UCLA School of Medicine, Cedars-Sinai Medical Center, 8700 Beverly Blvd, Los Angeles, CA 90048, Tel: (310) 423-4348, piotr.slomka@cshs.org

Abstract

Quantitative analysis of SPECT and PET has become a major part of nuclear cardiology practice. Current software tools can automatically segment the left ventricle, quantify function, establish myocardial perfusion maps and estimate global and local measures of stress/rest perfusion – all with minimal user input. State-of-the-art automated techniques have been shown to offer high diagnostic accuracy for detecting coronary artery disease, as well as predict prognostic outcomes. This chapter briefly reviews these techniques, highlights several challenges and discusses the latest developments.

Keywords

SPECT; PET; automated quantitation; myocardial function; left ventricular ejection fraction; myocardial perfusion; total perfusion deficit; ischemia

INTRODUCTION

Radionuclide myocardial perfusion imaging (MPI) with SPECT or PET is the most widely used technique for detecting coronary artery disease (CAD) in clinical practice.[1] Currently,

Corresponding Author: Piotr Slomka.

Conflicts of interest: None

one of the main advantages of nuclear techniques over other modalities such as stress echocardiography or cardiac MRI, is the development of standardized methods for automated quantitation. Automated analysis of three-dimensional SPECT and PET images is now routine for both clinical and research purposes. Current software can automatically segment the left ventricle (LV), quantify left ventricular ejection fraction (LVEF), establish myocardial perfusion maps and estimate global and local measures of stress/rest perfusion – all with minimal user input. These methods have demonstrated better reproducibility, and at least similar diagnostic accuracy as qualitative visual analysis by expert readers.

Furthermore, automated quantitation continues to be an active field of research with several recent developments. For example, new software that checks automated LV contours for potential errors has been shown to further reduce the level of human supervision required.[2] Another promising development has been the use of machine learning to integrate a combination of automated imaging parameters with clinical data for greater diagnostic accuracy, and prediction of prognostic outcomes on a personalized basis.[3,4] In this chapter, we briefly review the principles, strengths and limitations of current automated quantitation methods, and discuss some of these latest developments.

OVERVIEW OF QUANTITATIVE METHODS

Gated myocardial perfusion imaging (MPI) with SPECT or PET generates information on reversible perfusion defects, fixed perfusion defects, LV function, LV volumes, regional wall motion and thickening. Although visual interpretation for all these parameters is feasible, it is more time-consuming, less reproducible and ultimately more dependent on the observer's expertise than utilizing automated methods. It has been demonstrated that computer-based quantitation provides an important means of improving consistency of interpretation.[5] A number of validated software packages are available for automated quantification (QPS-QGS, Emory Toolbox, 4D-MSPECT and Wackers-Liu CQ)[6–9]and are distributed by the main vendors of nuclear medicine imaging equipment. The basic principles are similar for each of these software packages: after segmentation of the LV, normalized relative radiotracer uptake in reconstructed slices is quantitatively compared against normal data files.

LV segmentation

The first step in quantification of perfusion and function is segmentation of the LV from both gated and static reconstructed data. Segmentation of the myocardium may sometimes be challenging due to possible large perfusion defects, extra-cardiac activity, and image noise. Typically, the most common sources of incorrect automated contours are gut activity and incorrect definition of the valve plane (Figure 1). Nonetheless, current software tools allow accurate automatic definition of LV contours in up to 90%.[2] Incorrect segmentation in the minority of cases can result in spurious defects mimicking perfusion abnormalities, and therefore, some supervision by an experienced observer is still required during this step. However, this can be accomplished by an experienced technologist, prior to scan interpretation. Furthermore, recent software developments, which are discussed in this

review, can be used to check automated LV contours, allowing readers to target manual adjustment only to those studies flagged by the algorithm for potential errors.

LV Function

Using the endocardial surfaces from LV segmentation, a volume curve spanning the cardiac cycle can be generated. From the volume curve data, LV end-diastolic volume (EDV), LV end-systolic volume (ESV), LV ejection fraction (LVEF), cardiac output, myocardial mass and diastolic function parameters (peak and time to peak filling and ejection rates) can then be calculated. Several studies confirm strong agreement between gated MPI and reference standard measurements of quantitative LVEF and LV volumes.[7,10–15] This relationship is relatively independent of the isotope, protocol, standard, and algorithm used. Reproducibility and repeatability for LVEF and LV volumes have also been shown to be high.[16,17] With regards to cross-algorithm reproducibility, a number of studies confirm strong correlation between different approaches - but systematic differences in the measurements do exist, and therefore normal limits for the specific imaging approach are required.[15,18–20] Prognostic thresholds for LVEF, EDV, and ESV have also been reported for quantitative software.[21,22]

Myocardial Perfusion

Polar maps—Evaluating myocardial perfusion involves the detection of significant differences between stress and rest images. For the visual observer, this is only a subjective analysis and can be particularly challenging if the differences are subtle or if there are differences in stress and rest alignment. By contrast, automated software offers several objective quantitative measures of myocardial perfusion. After LV segmentation, the standard processing sequence for automated analysis involves extraction of myocardial count densities to polar map coordinates (typically the maximal values for a given polar map pixel), and subsequent comparison of polar map samples to normal limits (Figure 2).[5,11,23] Site- or protocol-specific normal limits are derived from a small number of visually normal studies from low-likelihood patients (20 to 40 is usually sufficient) in the local population.[23,24] For any given myocardial location, the image count can be used to grade the ***severity*** of hypoperfusion – based on the number of standard deviations (SD) below the lower limit of normal. Polar maps can then be plotted with severity mapped to a color scale, or as so-called “blackout maps” where all pixels below normal limits are blacked-out (Figure 3). Another advantage of this quantitative approach is that the use of common polar map coordinates for all subjects allows objective inter-subject comparison of relative count intensities, as the image counts in each study are normalized to a common level.

Quantitative parameters of perfusion—Various quantitative parameters can be derived from myocardial perfusion scans, and reported at a regional (per vascular territory) or global (per ventricle) level. These parameters are most commonly obtained by comparison to normal-limits. For example, the ***extent*** of a perfusion defect can be expressed as the percentage of pixels in the polar map for which severity is greater than a predefined statistical threshold (e.g. 2–2.5SD below normal limits). This measure reflect the size of the perfusion defect and it has been validated against delayed enhancement MRI for infarct imaging.[25]

Most commonly, a single parameter combining both pixel-based ***severity and extent*** is used to quantify the overall magnitude of hypoperfusion e.g. the total perfusion deficit (TPD) - as employed by Cedars-Sinai QPS module.[23] The difference in TPD at stress and rest (i.e. ischemic TPD) can be used to quantify ischemia. A similar concept to TPD is used by other quantification packages.

In addition, segmental perfusion scores for the American Heart Association (AHA) 17-segment model can be derived, based on the average defect severity in a given segment. Segments are assigned computed severity scores according to a 5-point scale: (0 = normal; 1= mildly abnormal; 2 = moderately abnormal; 3 = severely abnormal; 4 = absent).[26] Segmental scores can be summed per region, or for the whole myocardium, and the summed stress score (SSS), the summed rest score (SRS), and the summed difference score (SDS) can be derived, analogous to the scheme employed in the visual scoring. Several validation studies for these techniques have been reported, with angiography as the gold standard.[23,27–29]

Standard tools with the above general functionality for both SPECT and PET (but with some differences in the computational analysis methods) are available in all the main software packages available commercially.

Myocardial Blood Flow

Positron emission tomography can additionally be used to quantify absolute myocardial blood flow (MBF) and myocardial perfusion reserve (MPR) - and it is currently the noninvasive reference standard for these measures. Such analysis has been shown to improve diagnostic accuracy compared with relative perfusion analysis;[30,31] and recent studies have also demonstrated that an abnormal quantitative MPR is an independent predictor of an adverse prognosis.[32,33] Furthermore, quantitative measures of MBF provide unique information about the coronary microcirculation that is not available from non-quantitative methods.[34] MBF quantitation with PET is discussed in further detail in chapter 12.

Transient Ischemic Dilation

The transient ischemic dilation (TID) ratio is another quantitative measure which can be derived following automated LV segmentation.[35] It is calculated as the ratio of ungated post-stress LV cavity volume to that at rest. Abnormally high values of the TID ratio are associated with severe and extensive CAD.[36] It is debated as to whether an increased TID ratio reflects true stress-induced stunning of the left ventricle, or extensive sub-endocardial ischemia – or indeed a combination. TID ratio can be effective in avoiding the problem of underestimating disease extent, which is inherent in the assessment of relative perfusion defects – particularly with subjective visual analysis. For example, in one study, the sensitivity for detecting severe disease improved significantly (from 64% to 71%; $p<0.05$) when TID was combined with TPD.[37]

QUANTITATIVE ANALYSIS OF MPI IN PRACTICE

Diagnostic Accuracy

A recent study confirmed that diagnostic accuracy in terms of area under curve (AUC) for detecting CAD using the latest automated quantitative MPI methods, is at least similar or marginally superior to that achieved by expert visual readers.[38] The latter was true for both attenuation-corrected (0.92 vs. 0.90, $p<0.01$) and non-attenuation corrected data (0.91 vs. 0.87, $p<0.01$); and even when additional information such as patient age and symptom history (not used by the computer software) was revealed to the reader (Figure 4).

Prognostic Accuracy

Previously, a number of studies have demonstrated the prognostic value of standard visual scoring of MPI – but this has also been shown to be valid for automated quantitative parameters.[39–41] Cox models based on automated stress TPD have been shown to have similar prognostic performance for predicting cardiac death, as those based on expert visual analysis incorporating clinical information (AUC: 0.72 vs. 0.71).[42]

Ischemic Change

A particularly useful application for quantitative analysis is the estimation of subtle changes in ischemic burden during longitudinal follow-up of the same patient. This can provide a reliable objective measure of a patient's response to therapy. Whilst this can also be performed with visual assessment, small but clinically important improvements can be under-interpreted due to the subjective scoring of different readers. The most common approach using quantitative analysis is to report the difference in the overall quantitative parameter between repeat scans such as TPD – and this has shown good reproducibility and repeatability.[43,44]

Newer automated software can further refine longitudinal follow-up by analyzing serial stress/rest studies together in pairs - thereby eliminating errors associated with multiple comparisons to normal limits and variations in contour placements.[45,46] This approach also has the advantage that it does not require normal limits.

COURAGE Trial—In the nuclear sub-study of the COURAGE trial, quantitative analysis of perfusion was compared before and after two different treatment strategies (percutaneous coronary intervention (PCI) + medical therapy vs. medical therapy alone).[41] Greater reduction of ischemia (TPD: −2.7%) was shown in the group with PCI therapy than in the group with medical therapy alone (TPD: −0.5%; $p < 0.0001$). Such small group differences are harder to demonstrate with visual scoring due to greater inter and intra-observer variability.[47,48] Consequently, clinical trials based on visual analysis may require considerably larger patient cohorts to show significant differences between study groups.

Reproducibility

An important strength of quantitative analysis is the inherent reproducibility of the measurements. Lower variability directly translates to improved detection of true differences in hypoperfusion. The reproducibility of quantitative perfusion analysis has been compared

to visual analysis for a stress/and rest SPECT scan, repeated on the same day.[43] Quantitative measures of stress, rest and ischemic (stress-rest) defects were significantly more reproducible than visual scores, with smaller repeatability coefficients (stress: 3.3% vs. 4.8%; rest: 1.8% vs. 3.8%; ischemic: 3.2% vs. 4.3%; all p <0.002). Bland-Altman plots for repeated measures of visual stress and automated stress perfusion size are shown in Figure 5. These comparisons clearly demonstrate the advantages of the quantitative perfusion analysis over visual expert analysis.

Limitations of MPI quantification

Accuracy of quantitative perfusion analysis can be reduced by imaging artifacts, which can mimic true defects. Artifacts can be caused by patient motion, photon attenuation, misalignment of attenuation maps, or spillover of extra-cardiac activity. Expert visual readers can detect and ignore the majority of these artifacts; but as quantitative analysis is generally trained on visually normal, artifact-free data, it is more prone to false-positives. However, new developments such as automatic motion correction, and automatic recognition of misalignment based on myocardium-mediastinum mismatch show potential in overcoming this limitation.[49,50] Attenuation correction can be performed to reduce the effect of photon attenuation correction; however most MPI SPECT (MPS) systems are not equipped with the attenuation correction hardware. Methods which involve 2-position imaging have been proposed for mitigation of attenuation correction artifacts if attenuation correction is not available.[51] These methods are of particular use on newer dedicated cardiac SPECT scanners which often are not equipped with AC but can perform fast imaging, making 2-position imaging practical clinically.[52,53] Novel fast-MPS protocols have been adopted with 2 sequential scans in 2 patient positions (supine/upright or supine/prone – depending on the scanner), allowing differentiation of true perfusion defects from artifacts, if AC is not available;[53,54] however, they make visual reading more complex. The 2-position approach may also allow for detection of position-related artifacts, which may occur with limited field-of-view gantry of the new scanners.[55]

Another acknowledged limitation of the quantitative approach is the need for normal perfusion databases - specific to the scanner, tracer, acquisition algorithm and patient demographic - in order to establish valid normal limits for quantitative parameters. Such factors can all result in differing myocardial count distributions, resolution, photon attenuation, and scatter.

RECENT ADVANCES & FUTURE DIRECTIONS

Quality Control Flags - Towards Full Automation

The only element of human interaction required in quantitative MPI analysis is the potential adjustment of computer-generated contours during LV segmentation in a minority of cases. This manual interaction introduces user variability in an otherwise fully automated workflow. Therefore, in efforts to reduce the requirement for this step, a quality control (QC) algorithm for automatic identification of potentially incorrect contours has recently been developed.[2] This automated contour check algorithm derives 2 parameters to categorize segmentation failure: the ‘shape flag’ to detect mask-failure cases, and the ‘valve-plane flag’

to detect mitral valve plane over- or undershooting. This method has been shown to be very accurate for detecting both types of error (AUC: 1.00 and 0.96 respectively), compared to expert readers.[2] A follow-up study employing this technique in 995 rest/stress 99mTc-sestamibi MPI studies has shown it to be reliable in directing the attention of technologists to those contours that need manual correction – and in this way, with some refinement, we are one step closer to *fully* unsupervised automated perfusion scoring - without sacrificing accuracy.[38] Furthermore, enhanced automation of quantitative analysis enabled by such algorithms may allow accelerated quality control for clinical trials on a large scale.

Motion-frozen quantification of perfusion

Cardiac motion can lead to blurring, and therefore, most MPI protocols now utilize cardiac gating during acquisition. It has been suggested that analysis of only the end-diastolic images, can improve the detection of CAD - particularly in smaller hearts.[56] However, using end-diastolic images in isolation is not suitable for reliable computer quantification, since they only contain counts from a limited portion of the cardiac cycle. Therefore, quantification of perfusion has most commonly been performed on summed (added) image frames from all cardiac gates, without consideration for cardiac motion.

A novel “motion-frozen” display and quantification technique, utilizing all gated frames and taking cardiac motion into account, has therefore been developed to address this issue.[57] This technique eliminates image blurring due to cardiac motion, with noticeable improvement in image quality. “Motion-freezing” of perfusion data is accomplished by detection and subsequent motion tracking of the LV endo- and epicardial borders, with an established LV myocardial contour extraction algorithm such as QGS. Subsequently, 3D non-linear image warping is applied to all phases of the gated data, deforming each image phase to match the position of the end-diastolic phase (Figure 6). The warped images can be summed forming “motion-frozen” perfusion images. Such “motion-frozen” perfusion images have a visual appearance similar to the end-diastolic frames but are less noisy since they contain counts from all or most cardiac cycles.

Image quantification algorithms can use the motion information in polar map co-ordinates to derive cardiac motion-corrected polar maps. Therefore, “motion-frozen” quantification can be performed using polar maps that are created from individual polar map samples for each portion of the cardiac cycle, as defined by the gated 3D contours. Such “motion-frozen” perfusion quantification has been demonstrated to improve the diagnostic performance in obese patients and the improvement in image quality is likely to be most useful for resolving borderline findings in patients with high ejection fractions, in which cardiac-motion significantly reduces the image resolution.[58] Furthermore, as image resolution increases, cardiac motion becomes the dominant degrading effect - therefore this novel technique may be of greater importance for PET or future high-resolution SPECT imaging.

Machine Learning

Machine learning is a form of artificial intelligence that has proven to be a highly effective for prediction and decision-making in a multitude of disciplines including internet search engines, natural language processing and finance trending. Increasingly it is finding

applications in medicine - particularly in genomics, but more recently in risk assessment for various disease processes.[59–61] Fundamentally, it differs from traditional risk assessment methods by making no priori assumptions about causative factors, thus allowing for an unbiased exploration of all available data for patterns that predict a patient's individual risk.[61]

Quantitative parameters from automated analysis of MPI provide a rich source of objective reproducible cardiac data that can be mined with machine learning algorithms for highly accurate diagnostics and prognostic risk assessment. Recent studies applying to machine learning to automated MPI analysis have confirmed this postulation. For example, Arsanjani *et al.* integrated various parameters from automated analysis (TPD, ischemic changes, and ejection fraction changes between stress and rest) with a support vector machines algorithm to generate a diagnostic score for significant CAD which was significantly superior to any single parameter in isolation.[62] Moreover, further studies showed it is also possible to combine quantitative parameters with clinical parameters, akin to the integrative clinical scan analysis performed by physicians for both diagnostic and prognostic risk assessments.[4,63] A LogitBoost ensemble machine learning method trained in a 10-fold cross-validation experiment was compared to TPD and visual scores in a large study (n=1181) with correlating invasive angiography. When clinical and imaging information was provided to LogitBoost, it achieved a significantly higher diagnostic accuracy for detection of significant CAD (87%) than one of the expert readers (82%) or TPD (83%; $p<0.01$); and a higher AUC (0.94±0.01) than TPD (0.88±0.01) or 2 visual readers (0.89, 0.85; $p<0.001$) (Figure 7).[63] A similar method was to combine quantitative perfusion and function parameters with clinical parameters to predict early revascularization from MPI.[4]

These recent efforts utilizing machine learning methods dismiss the myth that the integrative characteristics of visual reading cannot be emulated with automated software.

CONCLUSION

Current tools for automated quantitative analysis are now readily available and in widespread use. These methods have been proven to be clinically robust with superior reproducibility and at least comparable diagnostic and prognostic performance compared to visual scoring – even by experts. Nonetheless, some challenges remain in the pursuit of a fully unsupervised quantitative approach. For example, LV segmentation still needs to be verified by a skilled operator; and multiple quantitative parameters may need to be reconciled by the thought processes of an expert reader for the final interpretation. However, recent developments in software and machine learning show that even these challenges can be overcome by the latest technology.

Acknowledgments

This research was supported in part by Grant R01HL089765 from the National Heart, Lung, and Blood Institute/ National Institutes of Health (NHLBI/NIH) (PI: Piotr Slomka). Its contents are solely the responsibility of the authors and do not necessarily represent the official views of the NHLBI.

REFERENCES

1. Salerno M, Beller GA. Noninvasive assessment of myocardial perfusion. Circ Cardiovasc Imaging. 2009; 2:412–424. [PubMed: 19808630]
2. Xu Y, Kavanagh P, Fish M, Gerlach J, Ramesh A, Lemley M, Hayes S, Berman DS, Germano G, Slomka PJ. Automated Quality Control for Segmentation of Myocardial Perfusion SPECT. J Nucl Med. 2009; 50:1418–1426. [PubMed: 19690019]
3. Arsanjani R, Xu Y, Dey D, Vahistha V, Shalev A, Nakanishi R, Hayes S, Fish M, Berman D, Germano G, Slomka PJ. Improved accuracy of myocardial perfusion SPECT for detection of coronary artery disease by machine learning in a large population. J Nucl Cardiol. 2013; 20:553–562. [PubMed: 23703378]
4. Arsanjani R, Dey D, Khachatryan T, Shalev A, Hayes S, Fish M, Nakanishi R, Germano G, Berman D, Slomka P. Prediction of revascularization after myocardial perfusion SPECT by machine learning in a large population. J Nucl Cardiol. 2014:1–8.
5. Slomka P, Xu Y, Berman D, Germano G. Quantitative analysis of perfusion studies: Strengths and pitfalls. J Nucl Cardiol. 2012; 19:338–346. [PubMed: 22302181]
6. Ficaro EP, Lee BC, Kritzman JN, Corbett JR. Corridor4DM: the Michigan method for quantitative nuclear cardiology. J Nucl Cardiol. 2007; 14:455–465. [PubMed: 17679053]
7. Garcia EV, Faber TL, Cooke CD, Folks RD, Chen J, Santana C. The increasing role of quantification in clinical nuclear cardiology: the Emory approach. J Nucl Cardiol. 2007; 14:420–432. [PubMed: 17679051]
8. Germano G, Kavanagh PB, Slomka PJ, Van Kriekinge SD, Pollard G, Berman DS. Quantitation in gated perfusion SPECT imaging: the Cedars-Sinai approach. J Nucl Cardiol. 2007; 14:433–454. [PubMed: 17679052]
9. Liu Y-H. Quantification of nuclear cardiac images: The Yale approach. J Nucl Cardiol. 2007; 14:483–491. [PubMed: 17679055]
10. Germano G, Kiat H, Kavanagh PB, Moriel M, Mazzanti M, Su H-T, Train KF Van, Berman DS. Automatic quantification of ejection fraction from gated myocardial perfusion SPECT. J Nucl Med. 1995; 36:2138. [PubMed: 7472611]
11. Faber TL, Cooke CD, Folks RD, Vansant JP, Nichols KJ, DePuey EG, Pettigrew RI, Garcia EV. Left ventricular function and perfusion from gated SPECT perfusion images: an integrated method. J Nucl Med. 1999; 40:650–659. [PubMed: 10210225]
12. Kumita S, Cho K, Nakajo H, Toba M, Uwamori M, Mizumura S, Kumazaki T, Sano J, Sakai S, Munakata K. Assessment of left ventricular diastolic function with electrocardiography-gated myocardial perfusion SPECT: comparison with multigated equilibrium radionuclide angiography. J Nucl Cardiol. 2001; 8:568–574. [PubMed: 11593221]
13. Bax JJ, Lamb H, Dibbets P, Pelikan H, Boersma E, Viergever EP, Germano G, Vliegen HW, de Roos A, Pauwels EKJ. Comparison of gated single-photon emission computed tomography with magnetic resonance imaging for evaluation of left ventricular function in ischemic cardiomyopathy. Am J Cardiol. 2000; 86:1299–1305. [PubMed: 11113402]
14. Chua T, Yin LC, Thiang TH, Choo TB, Ping DZ, Leng LY. Accuracy of the automated assessment of left ventricular function with gated perfusion SPECT in the presence of perfusion defects and left ventricular dysfunction: correlation with equilibrium radionuclide ventriculography and echocardiography. J Nucl Cardiol. 2000; 7:301–311. [PubMed: 10958271]
15. Faber TL, Vansant JP, Pettigrew RI, Galt JR, Blais M, Chatzimavroudis G, Cooke CD, Folks RD, Waldrop SM, Gurtler-Krawczynska E. Evaluation of left ventricular endocardial volumes and ejection fractions computed from gated perfusion SPECT with magnetic resonance imaging: comparison of two methods. J Nucl Cardiol. 2001; 8:645–651. [PubMed: 11725260]
16. Nakajima K, Nishimura T. Inter-institution preference-based variability of ejection fraction and volumes using quantitative gated SPECT with 99mTc-tetrofosmin: a multicentre study involving 106 hospitals. Eur J Nucl Med Mol Imaging. 2006; 33:127–133. [PubMed: 16193310]
17. Hyun IY, Kwan J, Park KS, Lee WH. Reproducibility of Tl-201 and Tc-99m sestamibi gated myocardial perfusion SPECT measurement of myocardial function. J Nucl Cardiol. 2001; 8:182–187. [PubMed: 11295696]

18. Nichols K, Santana CA, Folks R, Krawczynska E, Cooke CD, Faber TL, Bergmann SR, Garcia EV. Comparison between ECTb and QGS for assessment of left ventricular function from gated myocardial perfusion SPECT. J Nucl Cardiol. 2002; 9:285–293. [PubMed: 12032476]
19. Nakajima K, Higuchi T, Taki J, Kawano M, Tonami N. Accuracy of ventricular volume and ejection fraction measured by gated myocardial SPECT: comparison of 4 software programs. J Nucl Med. 2001; 42:1571–1578. [PubMed: 11585875]
20. Véra P, Koning R, Cribier A, Manrique A. Comparison of two three-dimensional gated SPECT methods with thallium in patients with large myocardial infarction. J Nucl Cardiol. 2000; 7:312–319. [PubMed: 10958272]
21. Sharir T, Germano G, Kavanagh PB, Lai S, Cohen I, Lewin HC, Friedman JD, Zellweger MJ, Berman DS. Incremental prognostic value of post-stress left ventricular ejection fraction and volume by gated myocardial perfusion single photon emission computed tomography. Circulation. 1999; 100:1035–1042. [PubMed: 10477527]
22. Sharir T, Kang X, Germano G, Bax JJ, Shaw LJ, Gransar H, Cohen I, Hayes SW, Friedman JD, Berman DS. Prognostic value of poststress left ventricular volume and ejection fraction by gated myocardial perfusion SPECT in women and men: gender-related differences in normal limits and outcomes. J Nucl Cardiol. 2006; 13:495–506. [PubMed: 16919573]
23. Slomka PJ, Nishina H, Berman DS, Akincioglu C, Abidov A, Friedman JD, Hayes SW, Germano G. Automated quantification of myocardial perfusion SPECT using simplified normal limits. J Nucl Cardiol. 2005; 12:66–77. [PubMed: 15682367]
24. Van Train KF, Areeda J, Garcia EV, Cooke CD, Maddahi J, Kiat H, Germano G, Silagan G, Folks R, Berman DS. Quantitative Same-Day Rest-Stress Technetium-99m-Sestamibi SPECT: Definition and Validation of Stress Normal Limits and Criteria for Abnormality. J Nucl Med. 1993; 34:1494–1502. [PubMed: 8355069]
25. Slomka PJ, Fieno D, Thomson L, Friedman JD, Hayes SW, Germano G, Berman DS. Automatic detection and size quantification of infarcts by myocardial perfusion SPECT: clinical validation by delayed-enhancement MRI. J Nucl Med. 2005; 46:728–735. [PubMed: 15872343]
26. Tilkemeier PL, Cooke CD, Ficaro EP, Glover DK, Hansen CL, McCallister BD. American Society of Nuclear Cardiology information statement: Standardized reporting matrix for radionuclide myocardial perfusion imaging. J Nucl Cardiol. 2006; 13:e157–e171. [PubMed: 17174793]
27. Ficaro EP, Fessler JA, Shreve PD, Kritzman JN, Rose PA, Corbett JR. Simultaneous transmission/emission myocardial perfusion tomography diagnostic accuracy of attenuation-corrected 99mTc-Sestamibi single-photon emission computed tomography. Circulation. 1996; 93:463–473. [PubMed: 8565163]
28. Wolak A, Slomka PJ, Fish MB, Lorenzo S, Acampa W, Berman DS, Germano G. Quantitative myocardial-perfusion SPECT: comparison of three state-of-the-art software packages. J Nucl Cardiol. 2008; 15:27–34. [PubMed: 18242477]
29. Xu Y, Fish M, Gerlach J, Lemley M, Berman DS, Germano G, Slomka PJ. Combined quantitative analysis of attenuation corrected and non-corrected myocadial perfusion SPECT: Method development and clinical validation. J Nucl Cardiol. 2010; 17:591–599. [PubMed: 20387137]
30. Ziadi MC, Williams K, Guo A, Renaud JM, Chow BJW, Klein R, Ruddy TD, Aung M, Garrard L, Beanlands RSB. Does quantification of myocardial flow reserve using rubidium-82 positron emission tomography facilitate detection of multivessel coronary artery disease? J Nucl Cardiol. 2012; 19:670–680. [PubMed: 22415819]
31. Fiechter M, Ghadri JR, Gebhard C, Fuchs TA, Pazhenkottil AP, Nkoulou RN, Herzog BA, Wyss CA, Gaemperli O, Kaufmann PA. Diagnostic value of 13N-ammonia myocardial perfusion PET: added value of myocardial flow reserve. J Nucl Med. 2012; 53:1230–1234. [PubMed: 22776752]
32. Kajander SA, Joutsiniemi E, Saraste M, Pietilä M, Ukkonen H, Saraste A, Sipilä HT, Teräs M, Mäki M, Airaksinen J. Clinical Value of Absolute Quantification of Myocardial Perfusion With 15O-Water in Coronary Artery DiseaseClinical Perspective. Circ Cardiovasc Imaging. 2011; 4:678–684. [PubMed: 21926262]
33. Herzog BA, Husmann L, Valenta I, Gaemperli O, Siegrist PT, Tay FM, Burkhard N, Wyss CA, Kaufmann PA. Long-Term Prognostic Value of 13N-Ammonia Myocardial Perfusion Positron Emission Tomography Added Value of Coronary Flow Reserve. J Am Coll Cardiol. 2009; 54:150–156. [PubMed: 19573732]

34. Camici PGCF. Coronary Microvascular Dysfunction. N Engl J Med. 2007; 356:830–840. [PubMed: 17314342]
35. Mazzanti M, Germano G, Kiat H, Kavanagh PB, Alexanderson E, Friedman JD, Hachamovitch R, Van Train KF, Berman DS. Identification of severe and extensive coronary artery disease by automatic measurement of transient ischemic dilation of the left ventricle in dual-isotope myocardial perfusion SPECT. J Am Coll Cardiol. 1996; 27:1612–1620. [PubMed: 8636545]
36. Weiss AT, Berman DS, Lew AS, Nielsen J, Potkin B, Swan HJC, Waxman A, Maddahi J. Transient ischemic dilation of the left ventricle on stress thallium-201 scintigraphy: a marker of severe and extensive coronary artery disease. J Am Coll Cardiol. 1987; 9:752–759. [PubMed: 3558976]
37. Xu Y, Arsanjani R, Clond M, Hyun M, Lemley M Jr, Fish M, Germano G, Berman DS, Slomka PJ. Transient ischemic dilation for coronary artery disease in quantitative analysis of same-day sestamibi myocardial perfusion SPECT. J Nucl Cardiol. 2012; 19:465–473. [PubMed: 22399366]
38. Arsanjani R, Xu Y, Hayes SW, Fish M, Lemley M, Gerlach J, Dorbala S, Berman DS, Germano G, Slomka P. Comparison of Fully Automated Computer Analysis and Visual Scoring for Detection of Coronary Artery Disease from Myocardial Perfusion SPECT in a Large Population. J Nucl Med. 2013; 54:221–228. [PubMed: 23315665]
39. Pazhenkottil AP, Ghadri J-R, Nkoulou RN, Wolfrum M, Buechel RR, Küest SM, Husmann L, Herzog BA, Gaemperli O, Kaufmann PA. Improved outcome prediction by SPECT myocardial perfusion imaging after CT attenuation correction. J Nucl Med. 2011; 52:196–200. [PubMed: 21270455]
40. Leslie WD, Tully SA, Yogendran MS, Ward LM, Nour KA, Metge CJ. Prognostic value of automated quantification of 99mTc-sestamibi myocardial perfusion imaging. J Nucl Med. 2005; 46:204–211. [PubMed: 15695777]
41. Shaw LJ, Berman DS, Maron DJ, Mancini GBJ, Hayes SW, Hartigan PM, Weintraub WS, O'Rourke Ra, Dada M, Spertus Ja, Chaitman BR, Friedman J, Slomka P, Heller GV, Germano G, Gosselin G, Berger P, Kostuk WJ, Schwartz RG, Knudtson M, Veledar E, Bates ER, McCallister B, Teo KK, Boden WE. Optimal medical therapy with or without percutaneous coronary intervention to reduce ischemic burden: results from the Clinical Outcomes Utilizing Revascularization and Aggressive Drug Evaluation (COURAGE) trial nuclear substudy. Circulation. 2008; 117:1283–1291. [PubMed: 18268144]
42. Xu Y, Nakazato R, Hayes S, Hachamovitch R, Cheng VY, Gransar H, Miranda-Peats R, Hyun M, Shaw LJ, Friedman J. Prognostic value of automated vs visual analysis for adenosine stress myocardial perfusion SPECT in patients without prior coronary artery disease: A case-control study. J Nucl Cardiol. 2011; 18:1003–1009. [PubMed: 21932154]
43. Xu Y, Hayes S, Ali I, Ruddy TD, Wells RG, Berman DS, Germano G, Slomka PJ. Automatic and visual reproducibility of perfusion and function measures for myocardial perfusion SPECT. J Nucl Cardiol. 2010; 17:1050–1057. [PubMed: 20963537]
44. Berman DS, Kang X, Gransar H, Gerlach J, Friedman JD, Hayes SW, Thomson LEJ, Hachamovitch R, Shaw LJ, Slomka PJ. Quantitative assessment of myocardial perfusion abnormality on SPECT myocardial perfusion imaging is more reproducible than expert visual analysis. J Nucl Cardiol. 2009; 16:45–53. [PubMed: 19152128]
45. Prasad M, Slomka PJ, Fish M, Kavanagh P, Gerlach J, Hayes S, Berman DS, Germano G. Improved Quantification and Normal Limits for Myocardial Perfusion Stress–Rest Change. J Nucl Med. 2010; 51:204–209. [PubMed: 20124046]
46. Slomka PJ, Nishina H, Berman DS, Kang X, Friedman JD, Hayes SW, Aladl UE, Germano G. Automatic quantification of myocardial perfusion stress–rest change: a new measure of ischemia. J Nucl Med. 2004; 45:183–191. [PubMed: 14960634]
47. Mahmarian JJ, Cerqueira MD, Iskandrian AE, Bateman TM, Thomas GS, Hendel RC, Moye LA, Olmsted AW. Regadenoson induces comparable left ventricular perfusion defects as adenosine: a quantitative analysis from the ADVANCE MPI 2 trial. JACC Cardiovasc Imaging. 2009; 2:959–968. [PubMed: 19679284]
48. Cerqueira MD, Nguyen P, Staehr P, Underwood SR, Iskandrian AE. Effects of age, gender, obesity, and diabetes on the efficacy and safety of the selective A2A agonist regadenoson versus adenosine in myocardial perfusion imaging: Integrated ADVANCE-MPI trial results. JACC Cardiovasc Imaging. 2008; 1:307–316. [PubMed: 19356442]

49. Matsumoto N, Berman DS, Kavanagh PB, Gerlach J, Hayes SW, Lewin HC, Friedman JD, Germano G. Quantitative assessment of motion artifacts and validation of a new motion-correction program for myocardial perfusion SPECT. J Nucl Med. 2001; 42:687–694. [PubMed: 11337561]
50. Chen J, Caputlu-Wilson SF, Shi H, Galt JR, Faber TL, Garcia EV. Automated quality control of emission-transmission misalignment for attenuation correction in myocardial perfusion imaging with SPECT-CT systems. J Nucl Cardiol. 2006; 13:43–49. [PubMed: 16464716]
51. Nishina H, Slomka PJ, Abidov A, Yoda S, Akincioglu C, Kang X, Cohen I, Hayes SW, Friedman JD, Germano G. Combined supine and prone quantitative myocardial perfusion SPECT: method development and clinical validation in patients with no known coronary artery disease. J Nucl Med. 2006; 47:51–58. [PubMed: 16391187]
52. Nakazato R, Slomka PJ, Fish M, Schwartz RG, Hayes SW, Thomson LEJ, Friedman JD, Lemley M Jr, Mackin ML, Peterson B. Quantitative high-efficiency cadmium-zinc-telluride SPECT with dedicated parallel-hole collimation system in obese patients: Results of a multi-center study. J Nucl Cardiol. 2014; 22:266–275. [PubMed: 25388380]
53. Nakazato R, Tamarappoo BK, Kang X, Wolak A, Kite F, Hayes SW, Thomson LEJ, Friedman JD, Berman DS, Slomka PJ. Quantitative upright–supine high-speed SPECT myocardial perfusion imaging for detection of coronary artery disease: correlation with invasive coronary angiography. J Nucl Med. 2010; 51:1724–1731. [PubMed: 20956478]
54. Duvall WL, Sweeny JM, Croft LB, Barghash MH, Kulkarni NK, Guma KA, Henzlova MJ. Comparison of high efficiency CZT SPECT MPI to coronary angiography. J Nucl Cardiol. 2011; 18:595–604. [PubMed: 21638154]
55. Fiechter M, Gebhard C, Fuchs TA, Ghadri JR, Stehli J, Kazakauskaite E, Herzog BA, Pazhenkottil AP, Gaemperli O, Kaufmann PA. Cadmium-zinc-telluride myocardial perfusion imaging in obese patients. J Nucl Med. 2012; 53:1401–1406. [PubMed: 22870823]
56. Taillefer R, DePuey EG, Udelson JE, Beller GA, Benjamin C, Gagnon A. Comparison between the end-diastolic images and the summed images of gated 99mTc-sestamibi SPECT perfusion study in detection of coronary artery disease in women. J Nucl Cardiol. 1999; 6:169–176. [PubMed: 10327101]
57. Slomka PJ, Nishina H, Berman DS, Kang X, Akincioglu C, Friedman JD, Hayes SW, Aladl UE, Germano G. “Motion-frozen” display and quantification of myocardial perfusion. J Nucl Med. 2004; 45:1128–1134. [PubMed: 15235058]
58. Suzuki Y, Slomka PJ, Wolak A, Ohba M, Suzuki S, De Yang L, Germano G, Berman DS. Motion-frozen myocardial perfusion SPECT improves detection of coronary artery disease in obese patients. J Nucl Med. 2008; 49:1075–1079. [PubMed: 18552133]
59. Singal AG, Mukherjee A, Joseph Elmunzer B, Higgins PDR, Lok AS, Zhu J, Marrero Ja, Waljee AK. Machine learning algorithms outperform conventional regression models in predicting development of hepatocellular carcinoma. Am J Gastroenterol. 2013; 108:1723–1730. [PubMed: 24169273]
60. Xiong HY, Alipanahi B, Lee LJ, Bretschneider H, Merico D, Yuen RKC, Hua Y, Gueroussov S, Najafabadi HS, Hughes TR, Morris Q, Barash Y, Krainer AR, Jojic N, Scherer SW, Blencowe BJ, Frey BJ. The human splicing code reveals new insights into the genetic determinants of disease. Science. 2015; 347(6218)
61. Waljee AK, Higgins PDR. Machine Learning in Medicine: A Primer for Physicians. Am J Gastroenterol. 2010; 105:1224–1226. [PubMed: 20523307]
62. Arsanjani R, Xu Y, Dey D, Fish M, Dorbala S, Hayes S, Berman D, Germano G, Slomka P. Improved accuracy of myocardial perfusion SPECT for the detection of coronary artery disease using a support vector machine algorithm. J Nucl Med. 2013; 54:549–555. [PubMed: 23482666]
63. Arsanjani R, Xu Y, Dey D, Vahistha V, Shalev A, Nakanishi R, Hayes S, Fish M, Berman D, Germano G, Slomka PJ. Improved accuracy of myocardial perfusion SPECT for detection of coronary artery disease by machine learning in a large population. J Nucl Cardiol. 2013; 20:553–562. [PubMed: 23703378]

KEY POINTS

1. One of the main advantages of nuclear techniques over other imaging modalities is the development of standardized methods for automated quantitation.
2. Current software can automatically segment the left ventricle quantify left ventricular ejection fraction, establish myocardial perfusion maps and estimate global and local measures of stress/rest perfusion – all with minimal user input.
3. Quantitative analysis of myocardial perfusion imaging has shown better reproducibility, and at least similar diagnostic accuracy as qualitative visual analysis by expert readers.
4. The accuracy of the quantitative perfusion analysis can be compromised by imaging artifacts, because they may mimic true abnormalities.
5. Recent advances such as automated contour checking and application of machine learning bring us closer to *fully* automated analysis with strong diagnostic and prognostic impact.

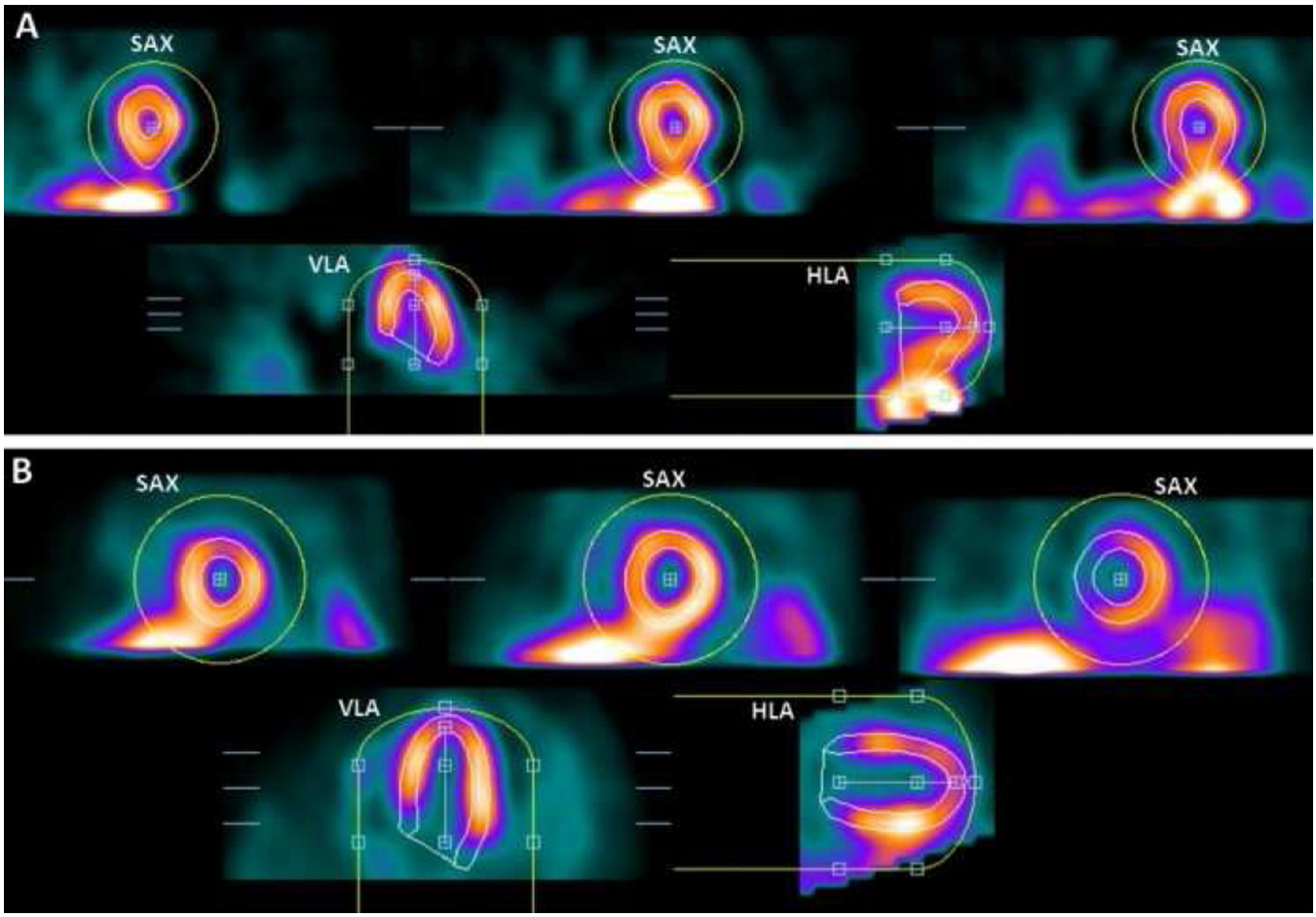

Figure 1. LV segmentation errors

In each image, top images are in short-axis orientation (SAX), and bottom images are in horizontal- and vertical (long)-axis orientation (HLA, VLA). Yellow circles show initial masks, and LV contours are shown in white. Panel (A) shows an example of mask-failure due to extracardiac activity. Panel (B) shows an example of valve-plane overshooting. *Adapted from* Xu Y, Kavanagh P, Fish M, et al. Automated Quality Control for Segmentation of Myocardial Perfusion SPECT. J Nucl Med 2009;50:1418–26; with permission.

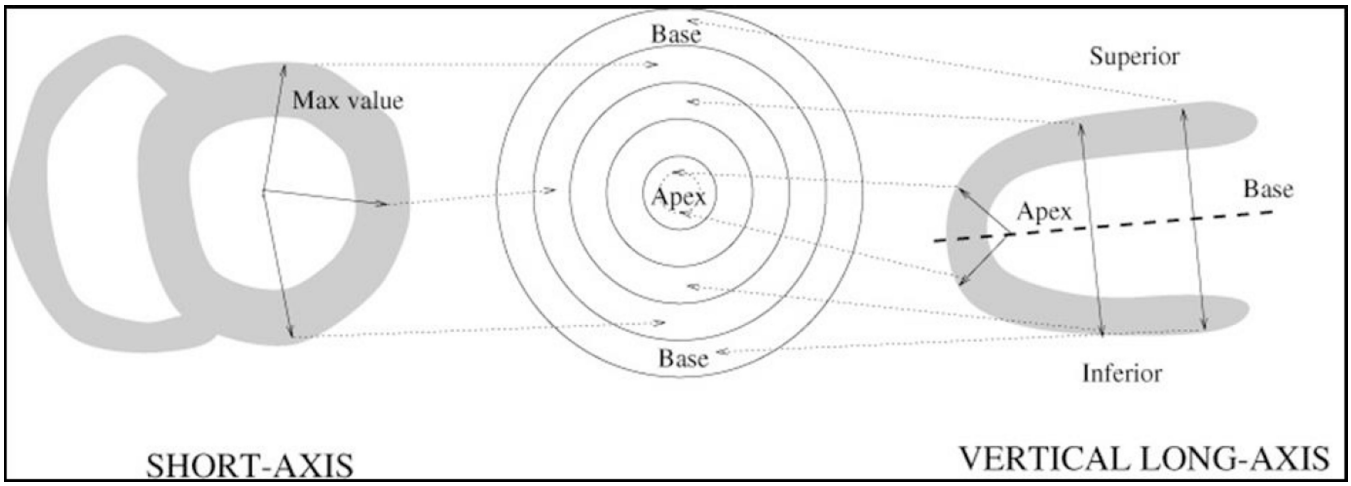

Figure 2. Polar map sampling of perfusion data

After LV segmentation, the standard processing sequence for automated analysis involves extraction of myocardial count densities to polar map coordinates.

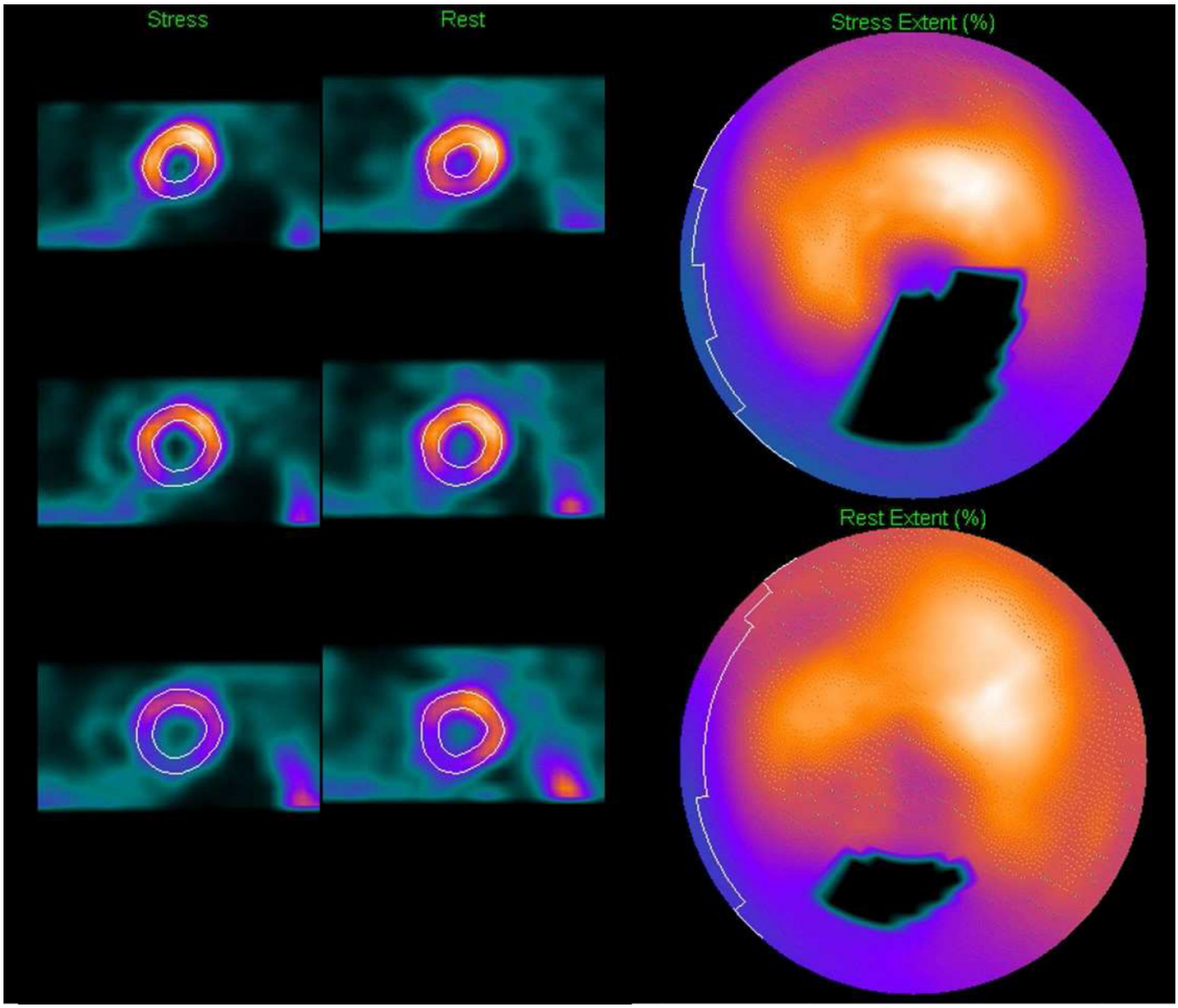

Figure 3. Blackout Maps

Blackout maps are derived by the quantitative software obtained by masking the polar maps pixels below normal limits. Corresponding short-axis stress (top right) and rest images (bottom right) are shown.

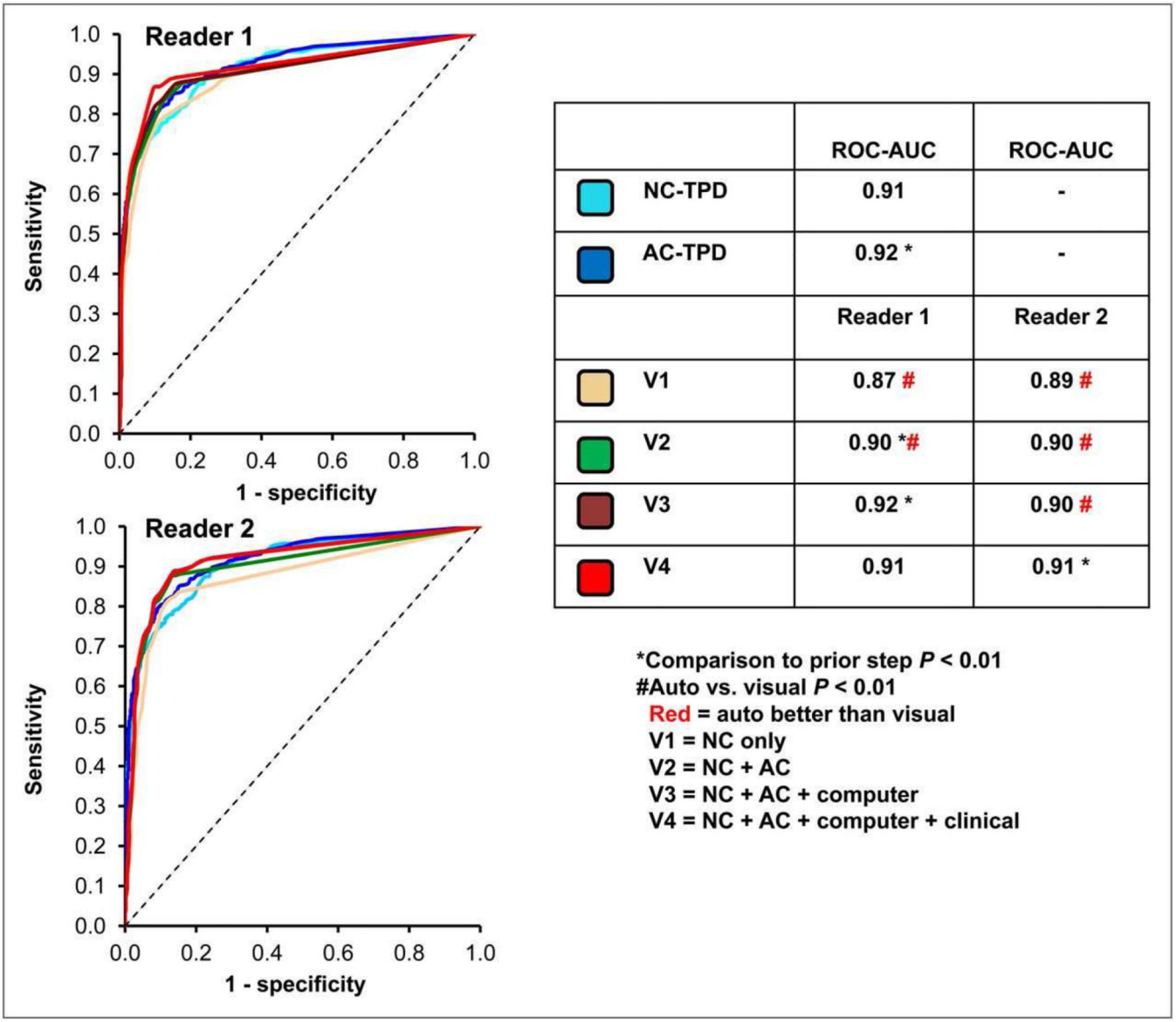

Figure 4. Receiver operating characteristic curves - automated versus visual analysis

A recent study confirmed that diagnostic accuracy for detecting CAD (≥70% stenosis) on a per-patient basis using automated methods is at least similar or marginally superior to that achieved by two expert visual readers. Comparisons were made for both attenuation corrected (AC) and non-attenuation corrected (NC) data, and using variable amounts of imaging and clinical data available to the reader (V1–V4).

From Arsanjani R, Xu Y, Hayes SW, et al. Comparison of Fully Automated Computer Analysis and Visual Scoring for Detection of Coronary Artery Disease from Myocardial Perfusion SPECT in a Large Population. J Nucl Med 2013;54:221–28; with permission.

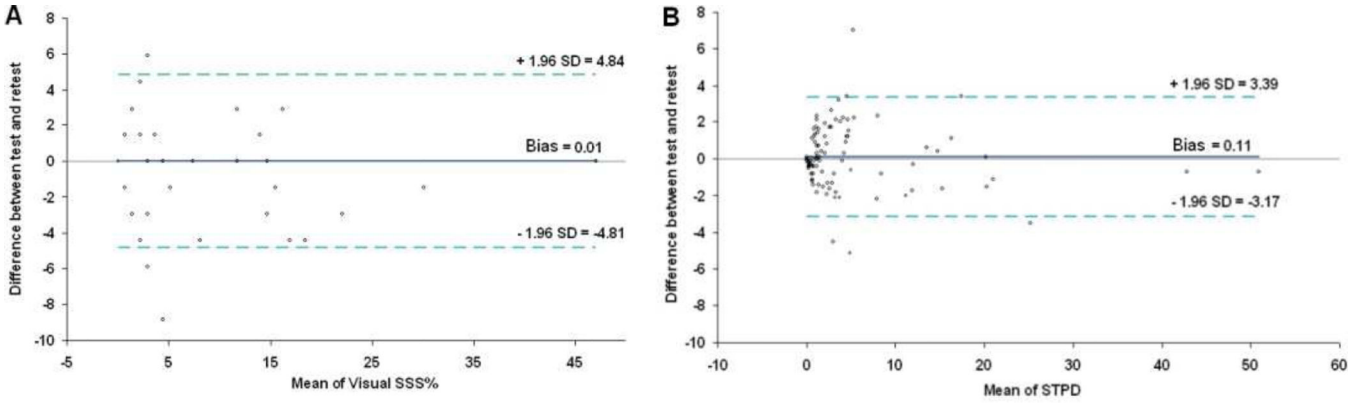

Figure 5. Reproducibility - automated versus visual analysis

Bland-Altman plots for visual (left) and automatic (right) repeated measurements of myocardial perfusion at stress are shown. The plot for automated stress total perfusion defect (STPD) shows better reproducibility with narrower limits of agreement compared to the plot for visual summed stress score as % of total myocardium (SSS%).

From Xu Y, Hayes S, Ali I, et al. Automatic and visual reproducibility of perfusion and function measures for myocardial perfusion SPECT. J Nucl Cardiol 2010;17:1050–7; with permission.

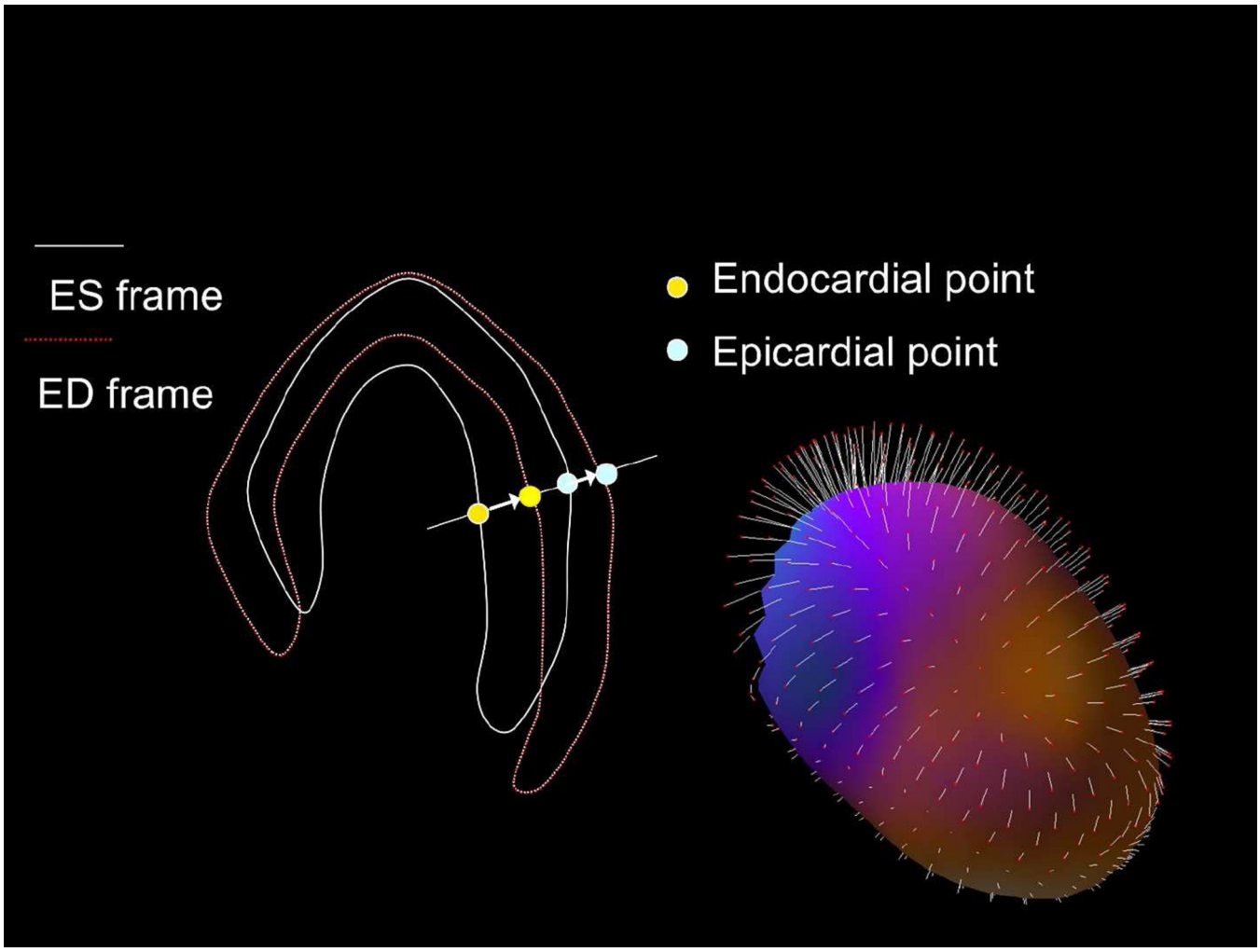

Figure 6. The principle of motion-frozen technique

Three-dimensional (3D) left ventricular (LV) contours are identified on images from different cardiac phases. End-systolic (ES – white) and end-diastolic (ED –red) frames are shown on the left. 3D phase to phase motion vectors are derived by sampling epi- and endocardial surfaces. 3D motion vectors are shown on the right, superimposed on epicardial surface of the LV ventricle. A non-linear image warping is than applied to warp all image phases to fit the ED phase.

Adapted from Slomka PJ, Nishina H, Berman DS, et al. "Motion-frozen" display and quantification of myocardial perfusion. J Nucl Med 2004;45:1128–34; with permission.

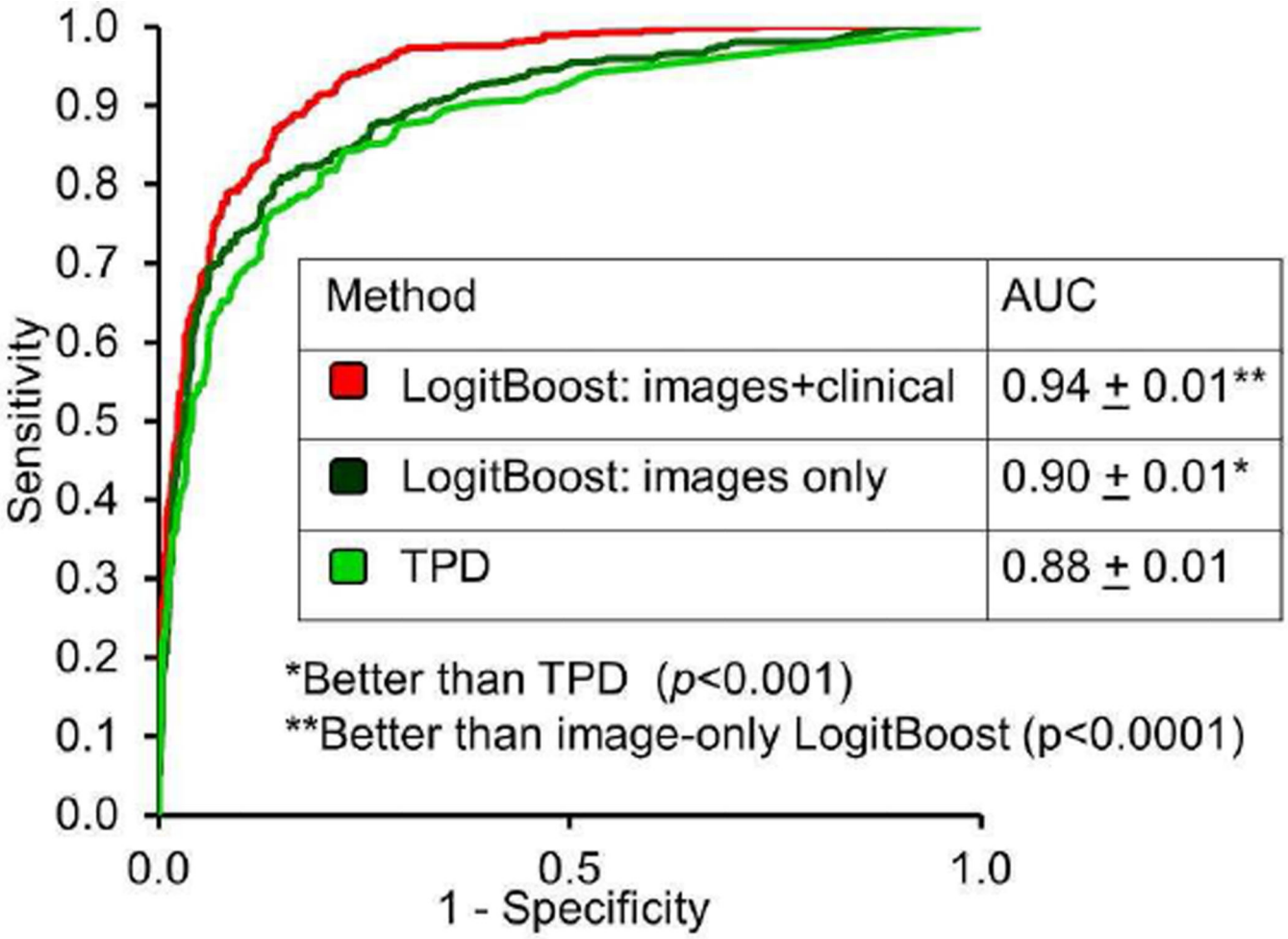

Figure 7. Application of machine learning to automated quantitation

When clinical and imaging information was provided to the LogitBoost machine learning technique in a large study (n=1181), it achieved a significantly higher diagnostic accuracy for detection of significant CAD (87%) than one of the expert readers (82%) or TPD (83%; P< 0.01); and a higher AUC (0.94±0.01) than TPD (0.88±0.01) or 2 visual readers (0.89,0.85;P < 0.001).

From Arsanjani R, Xu Y, Dey D, et al. Improved accuracy of myocardial perfusion SPECT for detection of coronary artery disease by machine learning in a large population. J Nucl Cardiol 2013;20:553–62; with permission.